

Timing of mineralization at the Shihu gold deposit in the middle segment of the Taihang Mountain, China

Chao Chen¹ · Shuyin Niu¹ · Fang Wang¹ · Fuxiang Zhang¹ · Qinglian Zhang¹ ·
Baojun Ma¹ · Aiqun Sun¹ · Jianzhen Zhang¹ · Yaqi Cao¹ · Xiaoqing Zhang¹

Received: 23 November 2016 / Revised: 17 March 2017 / Accepted: 7 April 2017 / Published online: 11 April 2017
© Science Press, Institute of Geochemistry, CAS and Springer-Verlag Berlin Heidelberg 2017

Abstract The Shihu gold deposit, located in the middle-south section of the core of the Fuping mantle branch structure, is hosted in the Archean Fuping Group and adjacent to the quartz diorite porphyry. The gold deposit is the only large gold deposit with reserves of more than 30 tons gold discovered in western Hebei Province so far. In order to constrain the timing of mineralization of this ore deposit, this paper focuses on the isotopic dating of zircon and pyrite. Zircons in gold-bearing quartz veins are magmatic in origin and no hydrothermal zircon has been found in such quartz veins, indicating that zircons were derived from the wall rocks. U–Pb ages of zircons fall mainly in the two domains: 2492 ± 82 and 136 ± 4 Ma, respectively, indicative of the contribution of the Fuping-Group TTG gneiss and Yanshanian igneous rocks, respectively. The Re–Os isotopic compositions of pyrites in the gold-bearing quartz veins yield an isochron age of 127 ± 31 Ma. Combined with other dating results, we suggest that the main metallogenetic age of the Shihu gold deposit is 120–127 Ma.

Keywords Mantle branch structure · Shihu gold deposit · Zircon U–Pb dating · Pyrite Re–Os dating · Gold-bearing quartz vein

1 Introduction

Precise and reliable metallogenetic ages are of important theoretical and practical significance in understanding the metallogenesis and ore-forming process, guiding ore

prospecting. Fortunately, great progresses have been made in direct isotopic dating technology, to the benefit of learning the mineralogenetic age of ore deposits (Mao et al. 2008; Zou et al. 2015; Yang and Zhou 2000; Zhang et al. 2002, 2009; Wang et al. 2013, 2014; Shi et al. 2012; Bi et al. 2008; Hu et al. 2004; Jiang et al. 2002; Zhao and Jiang 2004). However, all methods have limitations and uncertainties due to variable close temperatures of their isotopic systems. For example, the accuracy of Ar–Ar dating results of fluid inclusions in quartz and Rb–Sr isotopic dating for gold-bearing pyrite may be affected by later thermal events (Wang et al. 2013). Although the molybdenite Re–Os dating method was used to directly determine the ages of ore mineralization, the association of molybdenite and other sulfide minerals or big grains of molybdenite would generate different diffusions of Re and Os, leading to the decoupling of the Re–Os isotopic system and variable Os model ages. In addition, most of the quartz vein-type gold ores do not contain molybdenite. The U–Pb isotopes of zircons have relatively high closure temperatures ($>700^\circ\text{C}$) and can strongly resist hydrothermal disturbance, but the metallogenetic age of gold deposits may not be well determined by the U–Pb age of the zircon, because of the unclear origin of zircon from gold ore. Therefore, if one wants to precisely determine the mineralogenetic age, suitable dating methods should be adopted on the basis of the spatiotemporal relationship among various geological bodies of deposits.

The Shihu gold deposit belongs to the post-magmatic hydrothermal quartz vein-type-fault alteration rock-type gold deposits (Chen et al. 2009, 2011). More than 50 gold-bearing alteration zones have been found, and wall rocks are dominated by the adjacent quartz diorite porphyry and the Fuping Group. In regard to the mineralizing age of the Shihu gold deposit, Cao (2012) acquired the Ar–Ar dating of quartz and Rb–Sr isochron age of pyrite in the gold-

✉ Chao Chen
goldcc@163.com

¹ Hebei GEO University, Shijiazhuang 050031, China

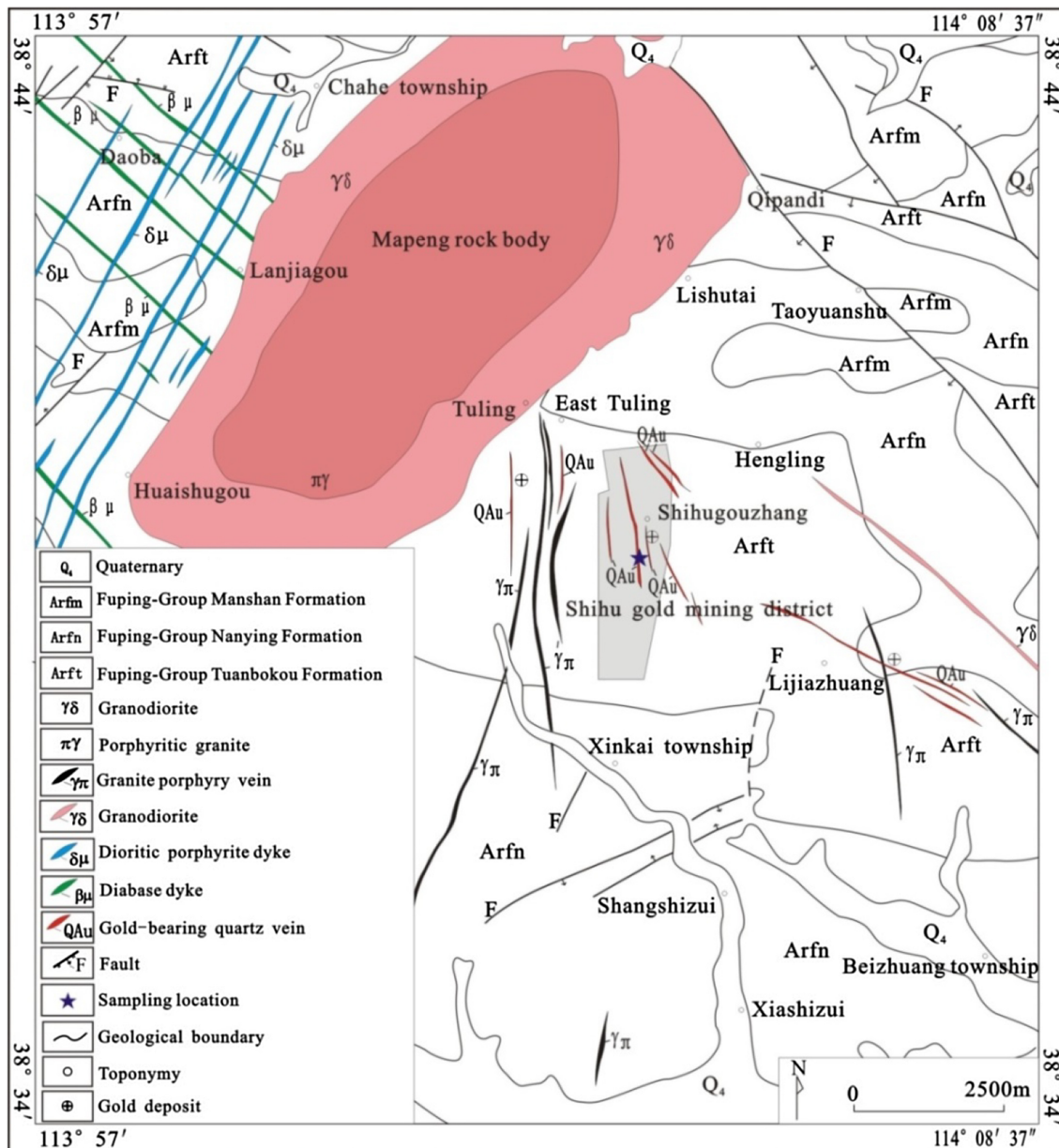


Fig. 1 The regional geological map of the Shihu gold deposit

bearing quartz veins as about 140 Ma. However, the U–Pb ages of quartz diorite porphyrite in host rocks and the Mapeng granite in this area have a formation age of 125–135 Ma (Liu et al. 2010a; Li et al. 2012a; Wang et al. 1995; Cao et al. 2012). Hydrothermal ore deposits of Shihu belong to epigenetic ones and would have minerallogenetic ages younger than those of wall rocks. It is not so suitable to regard the isotopic age of about 140 Ma as the main metallogenetic age. Therefore, the timing of gold mineralization at Shihu remains unclear.

In this paper, we carried out new zircon U–Pb and pyrite Re–Os isotopic dating of gold-bearing quartz veins with an attempt to comprehensively discuss the metallogenetic age of

the Shihu gold deposit. This can provide a good reference for further study on the gold and silver polymetallic metallocenic epoch in the Taihang Mountain.

2 Geological background

The Shihu gold deposit is located in the Taihang Mesozoic orogen of the North China Craton. According to the view of mantle branch structure, which is the third grade of structural units during the multiple evolutions of the mantle plume, put forward by Niu et al. (1996). It situates in the middle-south segment of the Fuping mantle branch structure in the

Taihang Mountain region, i.e., in the southern extension zone of the Zijinguang fault and on the south-eastern side of the Mapeng granite. The regionally exposed strata are mainly the moderately-high metamorphic rocks of the Manshan, Nanying and Tuanbokou formations of the Mesoarchean Fuping Group, petrologically dominated by biotite-plagioclase gneiss, leptite, plagioclase amphibolite, etc. The intrusive rockbodies in this region are mainly the Yanshanian intermediate-acid Mapeng rockbody which is exposed like a NE-extending shoe sole with an exposure area of about 65.0 km². There have been a large number of different types of dykes developed, which extend in different directions in the peripheries of the rockbodies, for example, NE-extending diorite porphyrite dykes, NW-extending dolerite dykes and nearly SN-extending granodiorite dykes. Tectonic activities are dominated by the Fupingian and Yanshanian activities. During the Fupingian stage there were formed the nearly EW-extending Chenzhuang complex fold structure and the ductile-deformation belt which extend in the same direction. On the basis of the development of the Early Yanshanian structure, the development of NNE-NE- and NW-extending fault tectonic systems followed. The fault structures are the important ore-forming structures in this region. There are a large number of Au–Ag deposits, forming an important base of metallic ores in the western Hebei Province (Fig. 1).

3 Ore deposit geology

In the Shihu gold deposit there are more than 50 gold-bearing alteration zones. Among them, No.101 and No. 116 ore veins are the major ones under mining. The No.101 gold vein nearly extends in the S–N direction with a E tendency or sleep W tendency, with a dip angle of 65°–90°. Extending length is over 4 km and the extending depth is up to 900 m. The occurrence of ore bodies is strictly controlled by the faults. The average thickness of ore bodies is 0.452–2.04 m and the gold grade is, in most cases, 3.52–27.9 g/t. The orebodies occur in vein- and lenticular shape with such features as obvious branching-recombination and thinning-out phenomenon. The occurrence of ore veins is closely associated with quartz diorite porphyrite (Fig. 2).

Ore minerals in this region are dominated by pyrite, galena, sphalerite, chalcopyrite, etc. The gangue minerals are mainly quartz, chlorite, sericite, plagioclase, K-feldspar, calcite, etc. Ore textures are mainly granular texture, disseminated texture, metasomatic relict texture, crush texture, etc. Ore structures are dominated by veinlet structure, disseminated structure, brecciated structure and massive structure. Gold occurs mainly in the form of electrum, kustelite or native gold embedded in sulfide minerals and quartz, with a particle size of 0.022–0.3 mm.

Interstitial gold, fracture gold and a small amount of encapsulated gold are the main occurrence of gold.

In this region there are a variety of wall-rock alterations, dominated by silicification, sericitization, beresitization, potassic alteration, chloritization, and locally developed carbonitization, etc. Alterations are distributed in the form of a belt. The closer to the ore bodies, the stronger the silicification, beresitization, and potassic alteration will become. Far from the ore bodies, carbonitization tends to become stronger and stronger.

4 Ore petrography

In order to obtain fresh quartz vein-type gold ore samples, the samples used in this analysis were collected from the No. 180 middle segment of the No. 101 vein in the Shihu gold deposit, and the sample numbers are Ysh1, Ysh4, Ysh7, Ysh8 and Ysh10. The quartz vein-type ores mainly show idiomorphic-hypidiomorphic granular texture, vein structure, brecciated structure, and veinlet structure. Polymetallic sulfides were

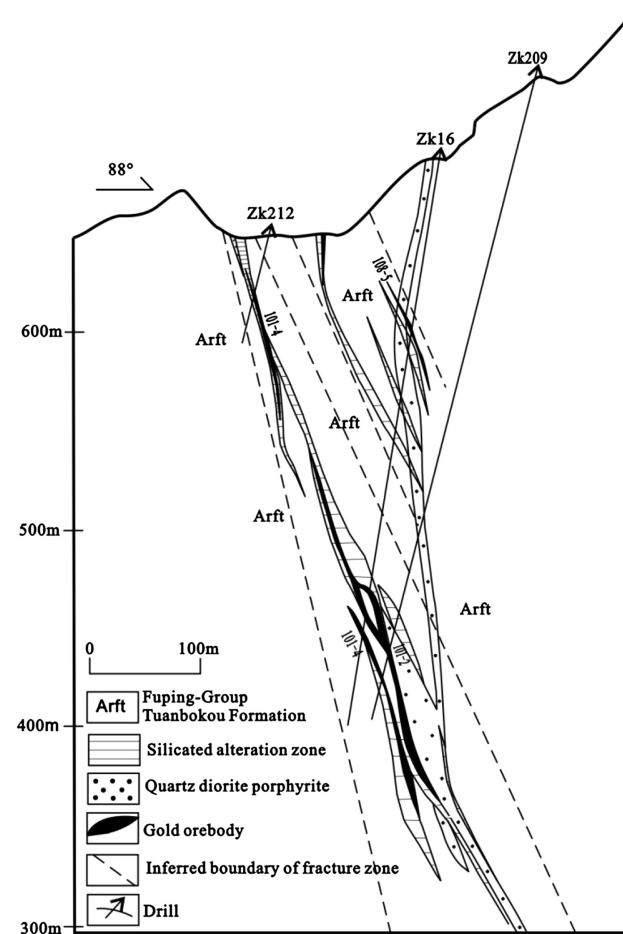
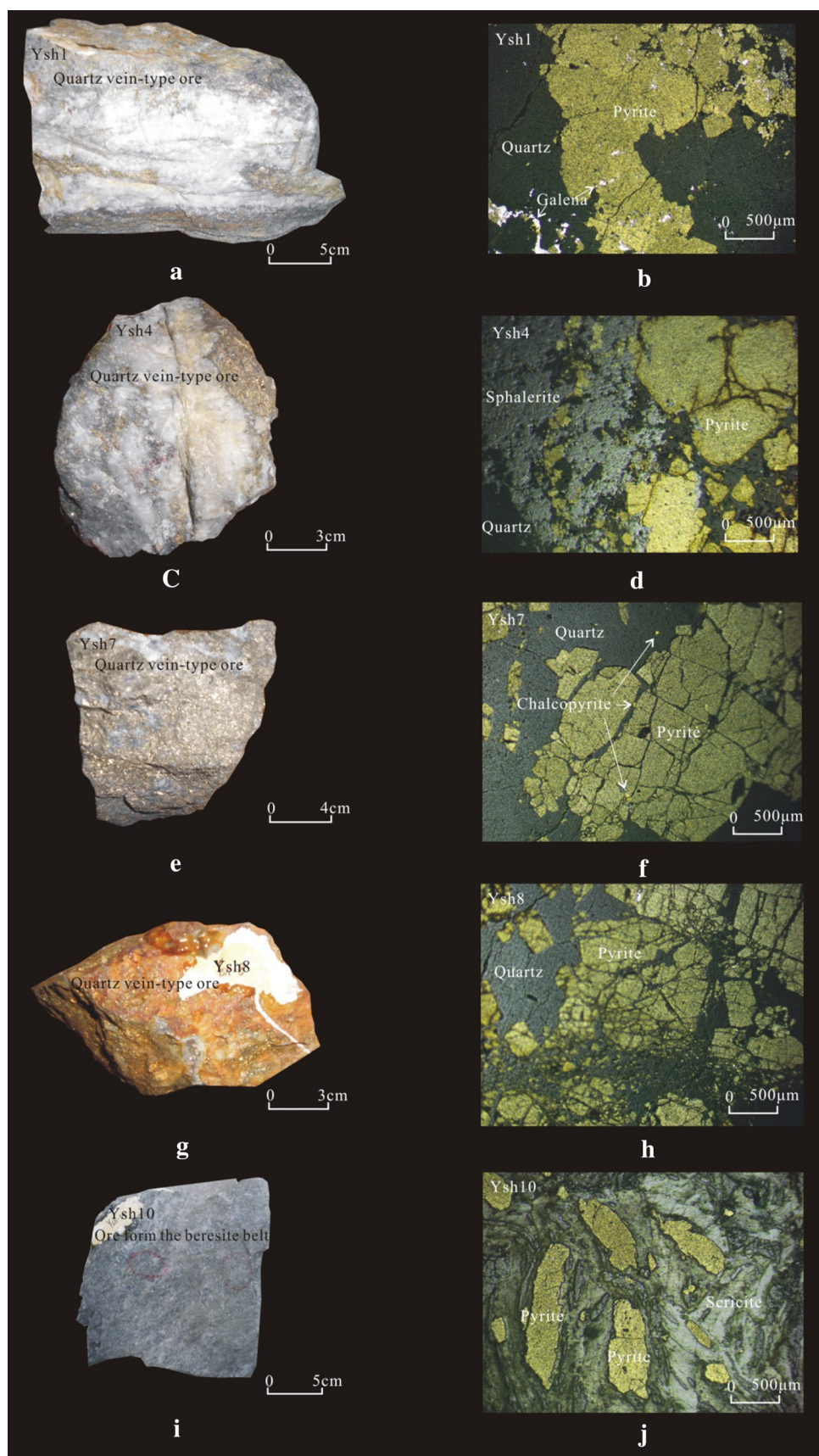


Fig. 2 The map of No.11 prospecting line profile of in No.101 gold ore vein the Shihu gold deposit

Fig. 3 Photographs of ore samples



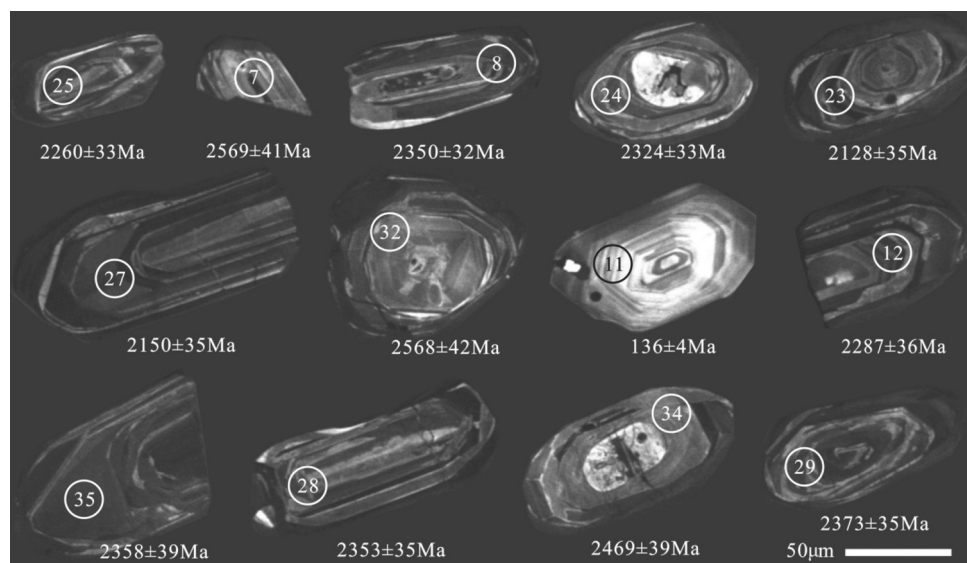
injected into the fissures of the siliconized belt. Meanwhile, relatively automorphic, coarse-grained nodular pyrite gravels (Fig. 3a, c) can be observed, indicating that there are at least two phases of pyrite. Ore minerals mainly include pyrite, galena, sphalerite, a small amount of chalcopyrite, etc. Most of the pyrites possess a subhedral-allotriomorphic texture and crush texture; galena and sphalerite have metasomatized pyrite, even wrapped rounded pyrite, and galena and chalcopyrite are distributed in the fissures of pyrite (Fig. 3b, d, f, h). All those phenomena indicate that pyrite was formed the earliest. The gangue minerals are dominated by quartz. The quartz can be divided into two types: one is represented by pure white quartz vein, which was always formed relatively early, and the other is represented by smoke-grey quartz which, together with metallic sulfide, constitutes fine-vein species occurring in the early-stage quartz veins (Fig. 3a). Ores in the pyrite-sericite-quartz rock belt have granular texture and massive structure. The main minerals are pyrite, quartz and sericite (Fig. 3i, j).

5 Analytical methods

5.1 Zircon U–Pb dating

In this study, sample Ysh1 was mainly used for zircon U–Pb dating. Zircon grains were separated by a standard heavy mineral separation technique, then zircons of different crystal forms, different colors and good transparency were chosen under the binoscope, fixed with polyepoxide on the glass plate, and then polished until the center. Before in situ analysis, the crystal morphology and inner textural features of zircons were carefully examined in terms of binocular and cathodoluminescence (CL) images, with an attempt to choose the best grains for isotopic analysis.

Fig. 4 Cathodoluminescence (CL) images of zircons in the gold-bearing quartz veins



Zircon U–Pb dating was conducted by a laser ablation inductively coupled plasma mass spectrometer (LA-ICP-MS) at the State Key Laboratory of Geological Processes and Mineral Resources, China University of Geosciences (Wuhan). Data processing of the test results was conducted by means of ICP-MS DataCal (Liu et al. 2008, 2010b, c), and zircon U–Pb concordia diagrams and the weighted age diagrams were prepared by using Software Isoplot/Ex_ver3 (Ludwig 2003).

5.2 Pyrite Re–Os dating

This study mainly aims at preparing and dating samples Ysh1, Ysh4, Ysh7, Ysh8 and Ysh10. The samples were crushed as fine as 40–60 mesh. Gold-carrying mineral-pyrite was hand-picked under the binocular microscope with a purity of more than 99% (no molybdenite was found in these ore samples). The chemical separation of the Re–Os isotopes in the pyrite samples and their mass spectrometric measurement were accomplished at the State Geological Experiment and Test Centre. The isotopic ratios were measured by means of inductively coupled plasma mass spectrometer (TJA X-series ICP-MS) following the procedure of Du et al. (1994, 2001). Regression analysis of the data results obtained was conducted by means of software Isoplot/Ex_ver3.

6 Analytical results

6.1 Zircon U–Pb dating

Zircon grains are colorless and transparent, and parts of them are clean and have no crack. Most of the zircon grains are elongated idiomorphic crystals and their cylindrical surfaces are well developed, the long axes are mostly between 60 and 100 μm with the length–width ratios being

Table 1 LA-ICP-MS U-Pb analysis results of zircons from gold-bearing quartz veins in the Shihu gold deposit

Analysis point	^{232}Th (10^{-6})	^{238}U (10^{-6})	Th/U	$^{207}\text{Pb}/^{206}\text{Pb} \pm 1\sigma$	$^{207}\text{Pb}/^{235}\text{U} \pm 1\sigma$	$^{206}\text{Pb}/^{238}\text{U} \pm 1\sigma$	$^{207}\text{Pb}/^{206}\text{Pb} \pm 1\sigma(\text{Ma})$	$^{206}\text{Pb}/^{238}\text{U} \pm 1\sigma(\text{Ma})$
YSH1-1	110.18	1017.47	0.11	0.1391 \pm 0.0036	3.9783 \pm 0.1153	0.2049 \pm 0.0037	2216 \pm 44	1201 \pm 20
YSH1-2	264.61	1370.36	0.19	0.1299 \pm 0.0032	4.1270 \pm 0.1332	0.2274 \pm 0.0053	2098 \pm 43	1321 \pm 28
YSH1-3	290.50	737.44	0.39	0.1571 \pm 0.0039	6.7506 \pm 0.2290	0.3068 \pm 0.0073	2424 \pm 43	1725 \pm 36
YSH1-4	203.67	943.74	0.22	0.1468 \pm 0.0036	6.0432 \pm 0.1938	0.2942 \pm 0.0063	2309 \pm 43	1662 \pm 31
YSH1-5	263.29	508.33	0.52	0.1477 \pm 0.0037	6.0548 \pm 0.2154	0.2927 \pm 0.0074	2319 \pm 43	1655 \pm 37
YSH1-6	173.07	771.27	0.22	0.1787 \pm 0.0047	6.9592 \pm 0.2430	0.2777 \pm 0.0060	2643 \pm 43	1580 \pm 31
YSH1-7	102.06	417.43	0.24	0.1711 \pm 0.0042	9.8432 \pm 0.3013	0.4129 \pm 0.0088	2569 \pm 41	2228 \pm 40
YSH1-8	38.37	599.49	0.06	0.1503 \pm 0.0033	9.3604 \pm 0.2895	0.4464 \pm 0.0106	2350 \pm 32	2379 \pm 47
YSH1-9	20.91	649.19	0.03	0.1504 \pm 0.0032	7.8742 \pm 0.2077	0.3757 \pm 0.0070	2350 \pm 37	2056 \pm 33
YSH1-10	263.80	1182.10	0.22	0.1260 \pm 0.0027	4.0554 \pm 0.1337	0.2294 \pm 0.0058	2042 \pm 39	1331 \pm 30
YSH1-11	134.89	392.18	0.34	0.0544 \pm 0.0037	0.1563 \pm 0.0100	0.0213 \pm 0.0007	387 \pm 152	136 \pm 4
YSH1-12	97.79	592.69	0.16	0.1448 \pm 0.0031	7.2422 \pm 0.2276	0.3592 \pm 0.0095	2287 \pm 36	1978 \pm 45
YSH1-13	201.63	857.89	0.24	0.1524 \pm 0.0031	6.0526 \pm 0.1705	0.2845 \pm 0.0058	2373 \pm 34	1614 \pm 29
YSH1-14	508.17	569.35	0.89	0.1648 \pm 0.0039	6.2539 \pm 0.1809	0.2779 \pm 0.0058	2505 \pm 41	1555 \pm 30
YSH1-15	490.22	2156.91	0.23	0.1240 \pm 0.0026	1.9560 \pm 0.0496	0.1122 \pm 0.0021	2014 \pm 38	686 \pm 12
YSH1-16	76.02	569.01	0.13	0.5353 \pm 0.0188	63.2974 \pm 3.8789	0.7728 \pm 0.0331	4342 \pm 46	3691 \pm 120
YSH1-17	116.06	490.32	0.24	0.1585 \pm 0.0031	8.4726 \pm 0.2192	0.3828 \pm 0.0068	2440 \pm 33	2089 \pm 32
YSH1-18	653.45	970.16	0.67	0.1434 \pm 0.0027	5.3490 \pm 0.1326	0.2679 \pm 0.0050	2269 \pm 33	1530 \pm 25
YSH1-19	44.58	1244.85	0.04	0.1171 \pm 0.0023	3.2471 \pm 0.0889	0.1990 \pm 0.0041	1922 \pm 35	1170 \pm 22
YSH1-20	28.86	279.53	0.10	0.1572 \pm 0.0030	10.6880 \pm 0.2593	0.4892 \pm 0.0093	2426 \pm 32	2567 \pm 40
YSH1-21	182.49	1248.45	0.15	0.1612 \pm 0.0050	3.5637 \pm 0.1540	0.1574 \pm 0.0037	2469 \pm 52	943 \pm 21
YSH1-22	191.19	654.50	0.29	0.1465 \pm 0.0028	5.8591 \pm 0.1428	0.2878 \pm 0.0055	2305 \pm 33	1630 \pm 27
YSH1-23	407.23	878.88	0.46	0.1321 \pm 0.0026	4.6036 \pm 0.1421	0.2507 \pm 0.0067	2128 \pm 35	1442 \pm 34
YSH1-24	50.13	496.62	0.10	0.1481 \pm 0.0029	6.7946 \pm 0.1842	0.3296 \pm 0.0068	2324 \pm 33	1836 \pm 33
YSH1-25	136.71	695.46	0.20	0.1428 \pm 0.0028	6.0909 \pm 0.1971	0.3064 \pm 0.0082	2261 \pm 33	1723 \pm 40
YSH1-26	969.45	1653.30	0.59	0.2216 \pm 0.0058	6.3967 \pm 0.2372	0.2056 \pm 0.0046	2992 \pm 43	1205 \pm 24
YSH1-27	433.03	1553.98	0.28	0.1338 \pm 0.0027	3.6649 \pm 0.1150	0.1953 \pm 0.0043	2150 \pm 35	1150 \pm 23
YSH1-28	79.49	657.56	0.12	0.1506 \pm 0.0031	7.3170 \pm 0.1917	0.3492 \pm 0.0065	2354 \pm 35	1931 \pm 31
YSH1-29	111.96	776.64	0.14	0.1523 \pm 0.0032	6.7234 \pm 0.1926	0.3169 \pm 0.0068	2373 \pm 35	1775 \pm 33
YSH1-30	261.97	1381.56	0.19	0.1306 \pm 0.0029	3.6691 \pm 0.1402	0.1962 \pm 0.0054	2106 \pm 40	1155 \pm 29
YSH1-31	222.54	1034.78	0.22	0.1524 \pm 0.0033	4.6586 \pm 0.1148	0.2197 \pm 0.0034	2373 \pm 37	1281 \pm 18
YSH1-32	160.08	537.94	0.30	0.1710 \pm 0.0043	8.6670 \pm 0.2413	0.3643 \pm 0.0060	2568 \pm 42	2003 \pm 28
YSH1-33	643.18	1337.82	0.48	0.1452 \pm 0.0033	3.9008 \pm 0.0985	0.1931 \pm 0.0030	2290 \pm 38	1138 \pm 16
YSH1-34	62.90	409.70	0.15	0.1613 \pm 0.0037	7.7900 \pm 0.2167	0.3473 \pm 0.0065	2469 \pm 39	1922 \pm 31
YSH1-35	217.13	1179.91	0.18	0.1510 \pm 0.0034	6.2063 \pm 0.1742	0.2950 \pm 0.0054	2358 \pm 39	1667 \pm 27
YSH1-36	189.64	405.98	0.47	0.1602 \pm 0.0038	9.0003 \pm 0.2636	0.4040 \pm 0.0081	2458 \pm 41	2187 \pm 37

smaller than 2. Their cathode luminescence is relatively strong, and the zircons mostly have obvious oscillatory zones. Within the zircons the oscillatory zones are wide and extend gently (Fig. 4).

Thirty-six zircon grains from sample Ysh1 were measured and analyzed (Table 1). The contents of Th and U are generally moderate with U contents varying within the range of 279×10^{-6} – 2157×10^{-6} , mainly between 406×10^{-6} and 1382×10^{-6} . Th contents vary within the range of 21×10^{-6} – 969×10^{-6} , mainly between 102×10^{-6} and 291×10^{-6} . Th/U ratios vary between 0.03 and 0.89, with an average of 0.27. For most zircon grains, their Th/U ratios are larger than 0.1. The zircons generally show the characteristic features of typical magmatic ones.

The data of only one point on sample Ysh1-16 were not taken into statistical calculation (Ysh1-16: the content of common lead is too high, and the age obtained is of incompatibility). The other values can be divided into two groups: one group of age data: the $^{207}\text{Pb}/^{206}\text{Pb}$ ages stand between 1922 ± 35 Ma and 2992 ± 43 Ma, mainly within the range of 2013 ± 37 – 2568 ± 41 Ma. The concordia diagram and weighted average age diagram were prepared respectively by using the age data with the concordia degrees $>80\%$ (Fig. 5). All data on the concordia diagrams are basically plotted below the concordant curve, indicating different degrees of lead loss. The age data constitutes, in general, a dissonance straight line with an upper intersection point of 2492 ± 82 Ma, standing for the crystallization age of the magmatic zircon. The weighted-average age is 2361 ± 33 Ma. This shows that this age and concordant age are reliable within a certain error range. The two groups of ages indicate that the crystallization age of zircon is close to the Late Neoarchean, within a certain error range. The second group of age data: the $^{206}\text{Pb}/^{238}\text{U}$ age of zircon

sample Ysh1-11 is 136 ± 4 Ma. And the zircon annules are clearly seen. Those zircons belong to magmatic ones, instead of the hydrothermal ones. Thus, zircons in the gold-bearing quartz veins are not crystallized from the Yanshanian hydrothermal fluids; instead, they were derived from the Fuping Group and Yanshanian magmatic rocks.

6.2 Pyrite Re–Os dating

Data of the Re–Os isotopic dating are presented in Table 2. Re content of pyrite sample Ysh10 among the 5 samples is too low, therefore the data of this sample were not taken into statistical calculation hereinafter. The data of the rest of the 4 samples lived up to the experiment requirements. Pyrite samples have Re ranging from 0.5276×10^{-9} to 1.1933×10^{-9} , common Os from 0.0004×10^{-9} to 0.0007×10^{-9} , and ^{187}Os from 0.0007×10^{-9} to 0.0019×10^{-9} . The contents of Re and Os in the pyrite samples are relatively low, yielding model ages with large errors (i.e., 115, 134 and 153 Ma). From the isochron age of pyrite Re–Os (Fig. 6), the $^{187}\text{Re}/^{188}\text{Os}$ and $^{187}\text{Os}/^{188}\text{Os}$ results of the four pyrite samples were fitted to a straight line and the isochron ages of 127 ± 31 Ma (MSWD = 192, initial $^{187}\text{Os}/^{188}\text{Os}$ ratio is 1.62 ± 0.26). The MSWD values obtained in this experiment are slightly high due to the low Re and Os contents of the pyrite samples used in this study.

7 Discussions

7.1 Age of wall-rock

The wall rocks of the Shihu gold ore veins are mainly the Archean Fuping Group biotite-plagioclase gneiss and

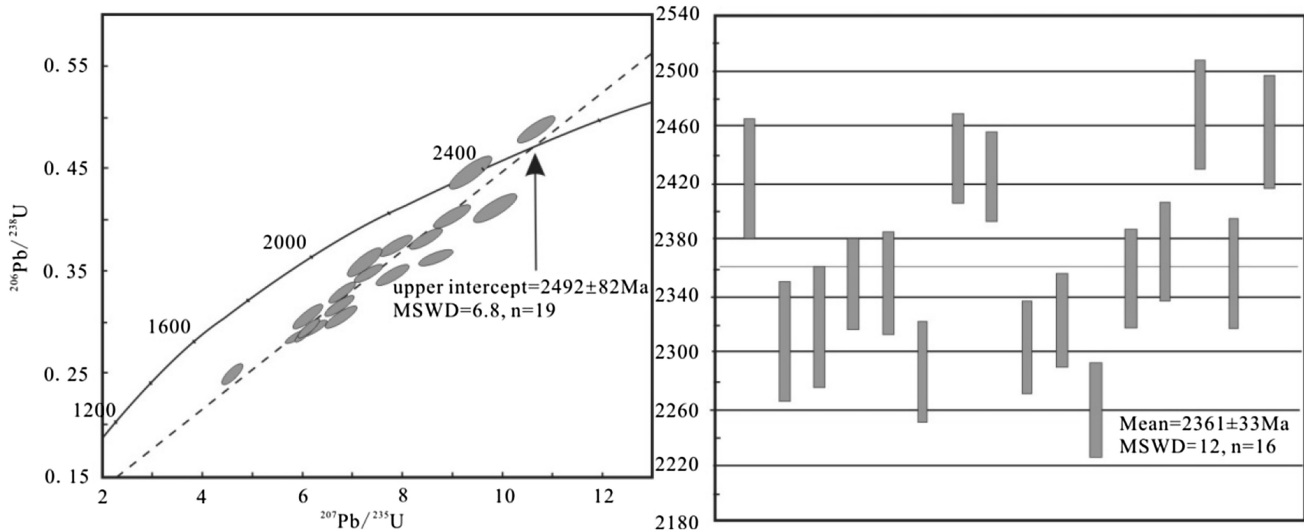
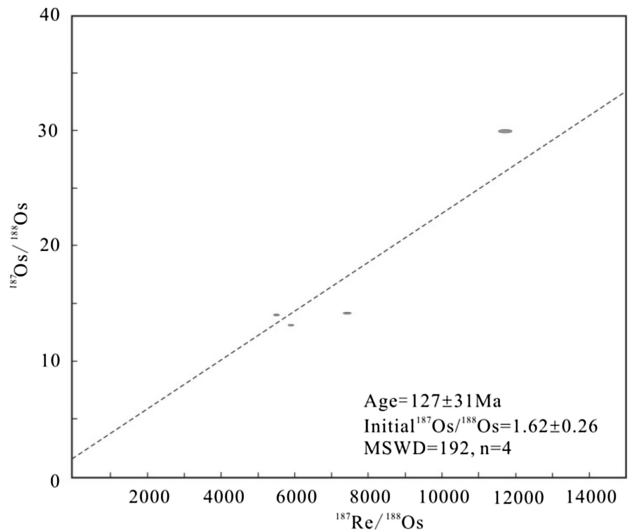


Fig. 5 Diagrams of U–Pb concordant ages and weighted average ages of zircons in gold-bearing quartz veins

Table 2 Results of Re–Os isotopic analysis for pyrites from the Shihu gold deposit

Original sample name	Sample quantity(g)	Re (ng/g)		Os _c (ng/g)		Re ¹⁸⁷ (ng/g)		Os ¹⁸⁷ (ng/g)		187 Os/188 Os		Model age (Ma)			
		Measured value	Uncertainty value	Measured value	Uncertainty value	Measured value	Uncertainty value	Measured value	Uncertainty value	Measured value	Uncertainty value				
Ysh-1	0.70332	0.9638	0.0072	0.0006	0.0000	0.6056	0.0045	0.0012	0.0000	7412	76	14,264	0.048	115.4	1.2
Ysh-4	0.60537	0.7914	0.0059	0.0007	0.0000	0.4975	0.0037	0.0013	0.0000	5504	58	14,085	0.046	153.4	1.6
Ysh-7	0.71044	0.5276	0.0039	0.0004	0.0000	0.3315	0.0025	0.0007	0.0000	5887	61	13,201	0.047	134.3	1.4
Ysh-8	0.71625	1.1933	0.0088	0.0005	0.0000	0.7499	0.0055	0.0019	0.0000	11705	122	29,936	0.094	153.7	1.6
Ysh-10	0.71088	0.1493	0.0011	0.0085	0.0001	0.0939	0.0007	0.0020	0.0000	85.14	0.87	1,803	0.005		

**Fig. 6** Re–Os isochron age plot of pyrites in the Shihu gold deposit

Yanshanian quartz diorite porphyrite dykes. The zircons of the gold-bearing quartz veins belong to magmatic ones and are likely originated from the surrounding rock. From the two groups' data of zircon U–Pb ages above, it can be realized that the upper intercept age of 2492 ± 82 Ma can be roughly representative of the Fuping Group age. The results are consistent with the reported data of Sun and Guan (2001), Guan et al. (2002), etc., that the Fuping group is mainly TTG (tonalite-trondhjemite-granodiorite) gneiss with a crystallization age of 2500 Ma ± (Late Neoarchean). Another $^{206}\text{Pb}/^{238}\text{U}$ age of 136 ± 4 Ma can represent the age of Yanshanian magmatic crystallization. The results are consistent with the data of Cao et al. (2012) that the LA-ICP-MS U–Pb zircon age of the quartz diorite porphyrite veins is around 130 Ma. This indicates that the zircons may be from quartz diorite porphyrite and gold-bearing quartz veins have assimilated some surrounding rock material.

In addition, as an important part of the tectonic-magmatic belt in the Taihang Mountain, the intermediate-acidic Mapeng granite is closely related to the endogenic metallic ore in the area. The emplacement activity of the intrusion has communicated the deep ore source and promoted the occurrence of mineralization (Chen et al. 2009, 2011). The rock-forming age of the Mapeng granite has been dated from 125 to 130 Ma zircon U–Pb dating (Cao et al. 2012; Li et al. 2012a; Liu et al. 2010a) and Wang et al. (1995) obtained a Rb–Sr isochron age of 135 Ma. This shows that the formation ages of the quartz diorite porphyrite and the Mapeng granite are very close. In addition, these two types of rocks have similar lithology, close temporospatial distribution, indicating that the age of 125–135 Ma in this area is a major magmatism event.

Table 3 Results of K–Ar isotopic analysis for feldspars in the Shihu gold deposit

Original sample name	Sample quantity(g)	K content(%)	$(^{40}\text{Ar}/^{38}\text{Ar})_m$	$(^{38}\text{Ar}/^{36}\text{Ar})_m$	$^{40}\text{Ar}^*$ (mol/g)	$^{40}\text{K}(\text{mol/g})$	$^{40}\text{Ar}^*/^{40}\text{Ar}(\%)$	$^{40}\text{Ar}^*/^{40}\text{K}$	Age(Ma)
Fsh-18	0.01083	10.14	397.89241	233.68186	2.196E−09	3.026E−07	98.37	0.0072558	120.74 ± 0.78

Analyzed by Petroleum Geological Experimental Research Centre of China Petroleum Exploration and Development Research Institute. The instrument model is MM5400 permanent vacuum mass spectrometer; $\lambda_e = 0.581 \times 10^{-10}\text{a}$; $\lambda_\beta = 4.962 \times 10^{-10}\text{a}$; $^{40}\text{K}/\text{K} = 1.167 \times 10^{-4}$ $^{40}\text{Ar}^*$, radiogenic argon

7.2 Timing of gold mineralization at Shihu

The Yanshanian quartz diorite porphyry is closely associated with gold veins. Within the broken belt and on its closely neighboring sides there can be developed quartz diorite porphyry dykes. In the ore veins, quartz- diorite porphyry breccias are associated with the development of disseminated and small vein-shaped sulfide veinlets. This indicates that the input of ore-forming fluids have crushed porphyry, thus leading to the transportation of ore fluids into fractures and gold precipitation in suitable locations. Such geological contact indicated that the timing of gold mineralization must be younger than the age of the ore-host quartz diorite porphyry.

Cao (2012) carried out the Ar–Ar isotopic dating of quartz in the gold-bearing quartz veins and the Rb–Sr isotopic dating of quartz and pyrite, obtaining ages around 140 Ma (the positive isochron age dated by the Ar–Ar method is 141 ± 4 Ma and the inverse isochron age is 139 ± 7 Ma; the age dated by using the Rb–Sr method is 139 Ma). However, analysis in combination with the ages of rock bodies in this region shows that the upper limit of metallogenetic age should be younger than 130 Ma. The zircon U–Pb ages in this study has revealed that gold-bearing quartz veins and gold mineralization are both formed later than 136 ± 4 Ma. The Re–Os isochron age of pyrite is 127 ± 31 Ma, consistent with the age (125–135 Ma) of the intrusions within error, indicating that the gold mineralization is related to the intrusion of igneous rocks.

Additionally, potassic alteration is always a common alteration type in the hydrothermal type gold deposits, which is closely related to gold mineralization. Therefore, the K–Ar isotopic dating of K-feldspar in the gold-bearing broken belt is of certain referring to the main metallogenetic age of gold deposits. This research group also conducted isotopic dating of K-feldspar (K–Ar method) in the No. 101 gold-bearing broken belt and obtained an isotopic age of 120.74 ± 0.78 Ma, close to the Re–Os isotopic age of pyrites within the range of experimental error (Table 3).

In combination with the geological relations and isotopic dating results (Ar–Ar, Rb–Sr, U–Pb, Re–Os, K–Ar), the main metallogenetic age of the Shihu gold deposit is

possible to be 120–127 Ma. This mineralogenetic age is relatively concordant to the time (130–110 Ma) when the event of lithospheric thinning in eastern China has caused the large scale gold mineralization in Jiaodong, Qinling, Taihang Mountain and other regions (Mao et al. 2003; Li et al. 2012b). According to the viewpoint of mantle branch structure (Niu et al. 1996, 2007), the time is the main evolution stage of Fuping mantle branch structure in the Taihang Mountain due to the multistage evolution of the mantle plume in the Yanshanian stage, causing the deep ore-forming materials to transfer from down to up and form the deposit at the favorable locations.

8 Conclusions

1. Two groups of U–Pb ages of zircons from quartz veins in the Shihu gold deposit have been obtained: 2492 ± 82 Ma and 136 ± 4 Ma, which respectively indicate that the crystallization age of the TTG gneiss in the Fuping Group and Mesozoic igneous rocks in the region.
2. The Re–Os isotopic dating of gold-bearing mineral-pyrite from quartz veins in the Shihu gold deposit yields an isochron age of 127 ± 31 Ma. In combination with the geological relations and K–Ar ages of K-feldspar in the No. 101 gold-bearing broken belt, it suggests that the main timing of gold mineralization is 120–127 Ma.

Acknowledgements This study was jointly funded by NSFC (No. 40872137), Hebei Natural Foundation (No. D2015403013), Science and Technology Research Project of Colleges and Universities in Hebei Province (No. ZC2016060) and Doctor Foundation of Hebei GEO University (No. BQ201320).

References

- Bi SJ, Li JC, Zhao XF (2008) Hydrothermal zircon U–Pb dating and geochronology of quartz vein-type gold deposits: a review. Geolo Sci Technol Inf 27(1):69–76
- Cao Y (2012) Mineralogical geochemistry and prediction for deep gold deposit in Shihu, western Hebei Province, North China. China University of Geosciences (Beijing) [Ph.D. Thesis], pp. 1–169

- Cao Y, Li SR, Xiong XX, Li ZZ, Liu XB, Yao MJ, Zhang HF (2012) Laser ablation ICP-MS U-Pb zircon geochronology of granitoids and quartz veins in the Shihu gold mine, Taihang Orogen, North China: timing of gold mineralization and tectonic implica. *Acta Geol Sin* 86(5):1211–1224
- Chen C, Niu SY, Wang BD, Sun AQ, Ma BJ, Wang WX, Gao YC (2009) A tentative discussion on ore-forming material sources and mineralization of the Shihu gold deposit in western Hebei Province. *Geol China* 36(6):1340–1349
- Chen C, Niu SY, Wang ZL, Guo Z, Sun AQ, Wang BD, Gao YC (2011) Comparison between the Xishimen gold deposit and the Shihu gold deposit in western Hebei and analysis of the potential for ore exploration. *Chin J Geochem* 30(3):281–289
- Du AD, He HL, Yin NW, Zou XQ, Sun YL, Sun DZ, Chen SZ, Qu WJ (1994) A study on the rhenium-osmium geochronometry of molybdenites. *Acta Geol Sin* 68(4):339–347
- Du AD, Zhao DM, Wang SX, Sun DZ (2001) Precise Re-Os dating for molybdenite by ID-NTIMS with carius tube sample preparation. *Rock Miner Anal* 20(4):247–252
- Guan H, Sun M, Wilde SA, Zhou XH, Zhai MG (2002) SHRIMP U-Pb zircon geochronology of the Fuping Complex: implications for formation and assembly of the North China craton. *Precambrian Res* 113:1–18
- Hu FF, Fang HR, Yang JH, Wan YS, Liu DY, Zhai MG, Jin CW (2004) Metallogenic age of Rushan gold deposit of auriferous quartz vein type, Jiaodong: SHRIMP U-Pb dationg on hydrothermal zircon. *Chin Sci Bull* 49(12):1191–1198
- Jiang SY, Ling HF, Yang JH, Zhao KD, Ni P (2002) New isotopic tracers for hydrothermal mineralization and ore genesis studies and direct dating methods of ore deposits. *Miner Depos* 21(Supplement):974–977
- Li LL, Han BF, Miao GJ, Shu GM, Chen JF, Yang JH, Yang YH, Zhang YB (2012a) Geochronology, emplacement depth and tectonic implications of the Mapeng-Chiwawu granitic pluton in Fuping Complex of the Taihang Mountains. *Acta Petrol Et Miner* 31(3):289–306
- Li WJ, Bi SJ, Selby D, Chen L, Vasconcelos P, Thiede D, Zhou MF, Zhao XF, Li ZK, Qiu HN (2012b) Giant Mesozoic gold provinces related to the destruction of the North China craton. *Earth Planet Sci Lett* 349–350:26–27
- Liu YS, Hu ZC, Gao S, Günther D, Xu J, Gao CG, Chen HH (2008) In situ analysis of major and trace elements of anhydrous minerals by LA-ICP-MS without applying an internal standard. *Chem Geol* 257:34–43
- Liu Y, Li CM, Zheng J, Huang FX, Sun H, Tang Y, Xu B (2010a) Zircon SHRIMP U-Pb age of Mapeng granite complex and its implication in Northern Taihang Mountains. *Geol Explor* 46(4):622–627
- Liu YS, Gao S, Hu ZC, Gao CG, Zong KQ, Wang DB (2010b) Continental and oceanic crust recycling-induced melt-peridotite interactions in the Trans-North China Orogen: U-Pb dating, Hf isotopes and trace elements in zircons of mantle xenoliths. *J Petrol* 51:537–571
- Liu YS, Hu ZC, Zong KQ, Gao CG, Gao S, Xu J, Chen HH (2010c) Reappraisal and refinement of zircon U-Pb isotope and trace element analyses by LA-ICP-MS. *Chin Sci Bull* 55(15):1535–1546
- Ludwig KR (2003) ISOPLOT 3.00: A geochronological toolkit for microsoft excel. California, Berkeley: Berkeley Geochronology Center, pp 39
- Mao JW, Zhang ZH, Yu JJ, Wang YT, Niu BG (2003) Mesozoic tectonic setting of large scale ore-forming in East China and adjacent areas: revealed by precise ages of metallic deposits. *Sci China Ser D* 33(4):289–299
- Mao GZ, Hua RM, Long GM, Lu HJ (2008) Discussion on the mineralogenetic epoch of the Jinshan gold deposit, Jiangxi Province: based on the quartz fluids inclusion Rb-Sr dationg. *Acta Geol Sin* 82(4):532–539
- Niu SY, Luo DW, Ye DH, Li HY, Wang JS (1996) Mantle branch structure and its metallogenetic regularity. Geological Publishing House, Beijing, pp 1–124
- Niu SY, Sun AQ, Wang BD (2007) Mantle plume and natural resources environment. Geological Publishing House, Beijing, pp 1–264
- Shi GY, Sun XM, Pan WJ, Hu BM, Qu WJ, Andao Du, Li C (2012) Re-Os dating of auriferous pyrite from the Zhenyuan super-large gold deposit in Ailaoshan gold belt, Yunnan Province Southwestern China. *Chin Sci Bull* 57(26):2492–2500
- Sun M, Guan H (2001) Zircon U-Pb ages of the Fuping Complex and their implication: some comments on the geochronological study of Precambrian high-grade metamorphic terranes. *Acta Petrol Sin* 17(1):145–156
- Wang QC, Ma JL, Zhang JZ (1995) Geochemical characteristics and genesis of Mapeng goldfield bordering Lingshou and Fuping, Hebei China. *Geochimica* 24(1):56–68
- Wang B, Zou YL, Chao YY, Yang YX (2013) Direct dating methods of gold deposits associated with hydrothermal mineralization. *Gold* 34(4):8–13
- Wang YT, Li X, Wang RT, Liu XL, Hu QQ, Li JH, Wang CA, Wen B, Wen SW, Wang SL (2014) Evidence of Ar-Ar Age for the metallogenetic epoch of Simaojing gold deposit in Fengxiao-Taibai ore cluster of Shanxi. *J Earth Sci Environ* 36(3):61–72
- Yang JH, Zhou XH (2000) Rb-Sr isochronic age and metallogenetic age of ore minerals and pyrites of the Linglong gold deposits Jiaodong area. *Chin Sci Bull* 45(14):1547–1553
- Zhang LC, Shen YC, Liu TB, Zeng QD, Li GM, Li HM (2002) Ar-Ar and Rb-Sr isochron ages and ore-forming time for gold deposits in northern margin of Jiaolai basin Shandong Province. *Sci China Ser D* 32(9):727–734
- Zhang XW, Xiang H, Zhong ZQ, Zhou HW, Zhang L, Yang N, Wang J (2009) U-Pb dating and trace elements composition of hydrothermal zircons from Jianfengling granite, Hainan: restriction on the age of hydrothermal event and mineralization of Baolun gold deposit. *Earth Science-Journal of China University of hydrothermal event and mineralization of Baolun gold deposit. Geosciences* 34(6):921–930
- Zhao KD, Jiang SY (2004) Direct isotope dating for metallic ore deposits. *Earth Sci Front* 11(2):425–434
- Zou YQ, Huang WT, Liang HY, Wu J, Lin SP, Wang XZ (2015) Identification of porphyry genetically associated with mineralization and its zircon U-Pb and biotite Ar-Ar age of the Xiongcun Cu-Au deposit, southern Gangdese Tibet. *Acta Petrol Sin* 31(7):2053–2062